A Two-dimensional Steady State Simulation Study on the Radio Frequency Inductively Coupled Argon Plasma

Ho-Jun Lee, Dong-Hyun Kim and Chung-Hoo Park

Abstract - Two-dimensional steady state simulations of planar type radio frequency inductively coupled plasma (RFICP) have been performed. The characteristics of RFICP were investigated in terms of power transfer efficiency, equivalent circuit analysis, spatial distribution of plasma density and electron temperature. Plasma density and electron temperature were determined from the equations of ambipolar diffusion and energy conservation. Joule heating, ionization, excitation and elastic collision loss were included as the source terms of the electron energy equation. The electromagnetic field was calculated from the vector potential formulation of ampere's law. The peak electron temperature decreases from about 4eV to 2eV as pressure increases from 5 mTorr to 100 mTorr. The peak density increases with increasing pressure. Electron temperatures at the center of the chamber are almost independent of input power and electron densities linearly increase with power level. The results agree well with theoretical analysis and experimental results. A single turn, edge feeding antenna configuration shows better density uniformity than a four-turn antenna system at relatively low pressure conditions. The thickness of the dielectric window should be minimized to reduce power loss. The equivalent resistance of the system increases with both power and pressure, which reflects the improvement of power transfer efficiency.

Keywords : inductively coupled plasma, plasma density, electron temperature, equivalent circuit analysis

1. Introduction

Low-pressure radio frequency inductively coupled plasmas are widely used as important sources for materials processing applications such as the etching of nano-structures and thin film deposition [1,2,3]. For the designing and manufacturing of the plasma systems for these applications, we must understand the effects of key design parameters and process variables on the system performances and plasma characteristics quantitatively. Although there have been many experimental and simulation studies on the RFICP, the investigations on the relationship between design parameters and characteristics of plasma systems are still quite limited. [4-9] With this background, we investigate the effect of process parameters and antenna configuration on the plasma characteristics such as electron density, temperature and equivalent impedance through simulation studies.

2. Modeling

The major parameters to be calculated in our simulations are spatial distributions of plasma density, electron temperature and power absorption. The considered neutral species is Argon. The control parameters are process pressure, total input power and the antenna geometry. Steady state plasma density and electron temperature were obtained from the following ambipolar diffusion and energy balance equations.[10]

$$-\nabla \cdot (D_a \nabla n) = \nu_i n \tag{1}$$

$$\nabla \cdot (-k_T \nabla (T_e)) = Q - \frac{3}{2} n_e k T_e \nu_e - \sum K_i \varepsilon_i \tag{2}$$

Here ν_i represents ionization frequency and k is the boltzman constant. At the boundary of the plasma chamber the electron density was set to zero. The ambipolar diffusion coefficient D_a is given as $0.5788 m^2$/ sec/P(Torr).[11]

The ionization and excitation frequency was given as follows. These are the fitted values from the data presented in reference [6].

$$\nu_i = 5.844 \times 10^{-14} N_n \cdot T_e^{0.283} \exp(\frac{-16.22}{T_e})$$

$$\sum K_i \varepsilon_i = 11.6(eV) \cdot N_n \cdot n_e \cdot 3.71 \times 10^{-14} \cdot T_e^{0.0745} \exp(\frac{-12.14}{T_e})$$

Here, N_n is neutral particle density and T_e is in the eV unit. The ambipolar diffusion approximation assumes that the ion and electron flux is balanced at each local position.

This work was supported by Korean Research Foundation Grant (KRF-99-E00155).

Manuscript received: June 11, 2002 accepted: Aug. 26, 2002

Ho-Jun Lee, Dong-Hyun Kim, Chung-Hoo Park are with the Deparment of Electrical Engineering, Pusan National University. Mt. 30 Jangjeon dong, Keum-jung Gu, Pusan, 609-735, Korea.

It is equivalent to a quasi-neutral plasma approximation. In this case, we can have a very fast simulation at the expense of the accuracy of the electron and ion density profile and information on the plasma potential distribution. However, at low pressure with a finite chamber dimension the applicability of this model breaks down because the potential distribution cannot be neglected. This can be resolved by two fluid treatments accounting for a curl-free electric field.

Equation (2) represents the balance between conductive heat flux and energy gain (or loss). A Neumann type boundary condition $\frac{\partial T_e}{\partial n} = 0$ was applied. The physical meaning of the condition is that all the power is consumed within the chamber and there is no heat flux outgoing from the vessel. k_T is the thermal conductivity.

$$k_T = \frac{5}{2} k n_e \frac{kT_e}{m_e \nu_m}$$

The source terms of equation (2) consist of ohmic heating, elastic and inelastic energy loss terms. For inelastic loss, both ionization and excitation energy loss are included. The energy relaxation frequency ν_e is given as a function of temperature and mass of the electrons and neutral atoms.[12]

$$\nu_e = \delta \nu_m (T_e - T_n),\ \delta = 2m_e/M$$

The temperature of neutral particles T_n was assumed to be 300K. The ohmic heating can be obtained from the electric field and conductivity of the plasma.

$$Q = \frac{1}{2} \mathrm{Re}(\sigma) E^2$$

$$\sigma = \frac{q_0^2 n_e}{m_e} \frac{1}{\nu_m + j\omega}$$

Here ν_m and ω are electron-neutral collision frequency and excitation angular frequency ($2\pi \times 13.56 \times 10^6$rad/sec) respectively. It should be noted that the conductivity used in this paper could deal with only the collisonal heating of electrons. However, in a low-pressure region with $\nu_m < \omega$ ($\nu_m = \omega$ at about 25mTorr for 13.56MHz) collisionless heating becomes important if the electron temperature is high enough for the electrons to travel the distance characterized by the scale length of the field inhomogeneity within a period of the time varying field. Therefore, the power absorption results presented here are somewhat underestimated for the low-pressure conditions. A detailed analysis on the collisionless heating can be found in ref.[13][14].

The induced rf electric field was calculated from the vector potential formulation of Ampere's law, which can be written as

$$\nabla \times (\frac{1}{\mu} \nabla \times \vec{A}) = -j\omega\sigma\vec{A} + J_{ext} \qquad (3)$$

$$\vec{E} = -j\omega\vec{A}$$

J_{ext} is the external current source. At the outmost domain boundary, a perfect magnetic insulation condition was applied. This means a perfect shielding of the rf field.

Fig. 1 shows the schematic diagram of the simulation flow. The plasma module returns conductivity to the electromagnetic (EM) module and the EM module returns power absorption. The EM module checks the total power absorbed and compares it with the desired power level given as an input parameter, and updates the source current density. After a few iterations, we could obtain self-consistent solutions. The differential equations were solved by using high level language based on the FEMLAB.[15]

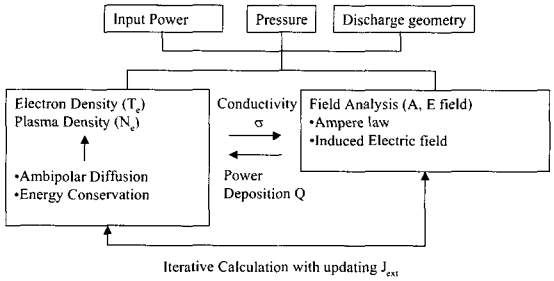

Fig. 1 Schematic diagram of the simulation flow

Fig. 2 shows the model geometry used in our study. The cylindrical vessel consists of an rf shielder, rf window and antenna for power coupling. Two types of antennae, single-turn and four-turn, were applied. The diameter and height of the plasma chamber are 15cm and 20cm respectively. Although the multi-turn antenna is spiral type in reality, we modeled it as concentric circular loops. Since the vector potential produced by the circular current loops has only an azimuthal component and plasma conductivity is isotropic, the vector potential throughout the calculation domain and induced electric field inside the plasma also have azimuthal component A_θ only.

3. Results and Discussions

3.1 Spatial Distributions of Plasma Parameters

Fig. 3 shows the spatial distributions of plasma density (a), electron temperature (b), power absorption (c), and ionization rate (d) for the condition of pressure 10 mTorr and power 500 W. Power absorption occurs near the dielectric window and antenna, which reflects the profiles of rf electric field intensity and skin effect. The maximum power transfer was about 1.6 W/cm^3. Although the power absorption is severely localized, the electron temperature variation throughout the chamber shows only about 20% due to heat transport. Plasma density at the center is 3×10^{10}/cm^3. The location where the highest ionizations occur is shifted 10cm from the center due to the electron

temperature distribution.

The maximum generation rate for this condition is about 5×10^{16}/sec/cm^3. Figs. 4 (a) and (b) are distribution of electron density and temperature for a higher pressure condition, 50 mTorr. As the pressure is increased, the diffusion coefficient becomes smaller and the location of the peak electron density moves closer to the antenna. The electron temperature shows more localized profiles as compared with the low-pressure condition.

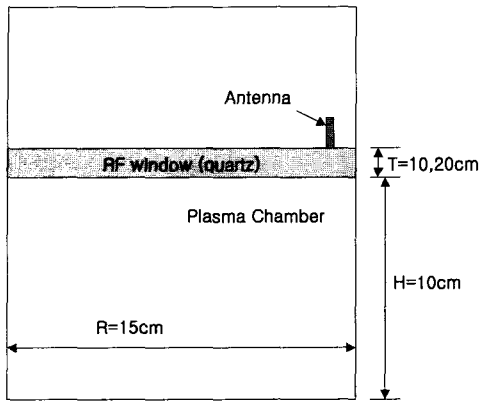

Fig. 2 Schematic diagram of the system

Although the ambipolar diffusion coefficient primarily depends on the pressure, it is a function of T_e also. However, judging from the results, the variation of T_e is only about a factor of two while pressure varies by order of magnitude. So it can be said that T_e gives a rather minor effect compared with pressure. For the spatial variation of T_e, it varies about 10% (at low pressure) to 40% (at high pressure). If we include T_e dependency, we then have a little lower density at a lower pressure condition and a little more flattened density profile at a higher pressure because the diffusivity near the power deposition region is higher. However, the general trend and profile will never be changed.

In case of four-turn antenna system the shape of constant-temperature contour, as shown in Fig. 5 (b), is wider in the radial direction than that of the single antenna system, which reflects the broadening of the power absorption

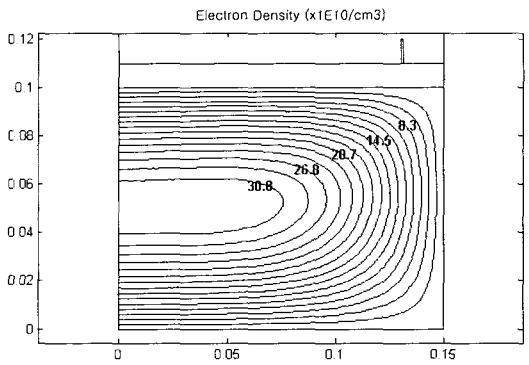

Fig. 3(a) Spatial Distribution of Electron Density(10 mTorr, 500W)

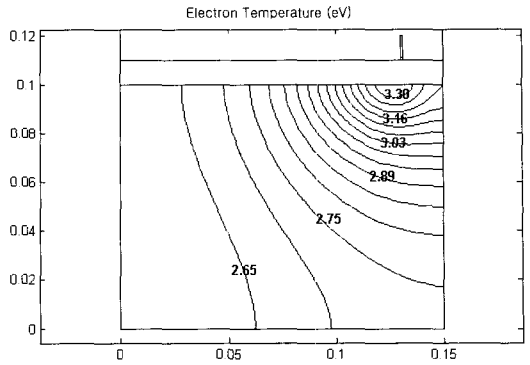

Fig. 3(b) Spatial Distribution of Electron Temperature (10 mTorr, 500 W)

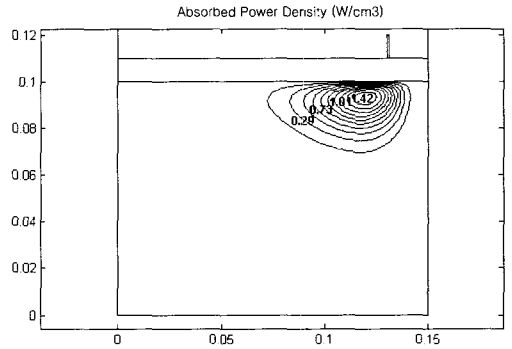

Fig. 3(c) Absorbed Power Density (10 mTorr, 500 W)

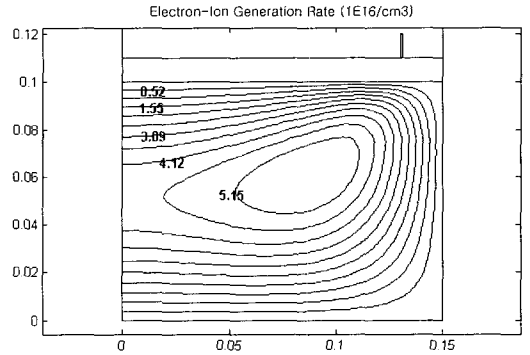

Fig. 3(d) Spatial Distribution of Electron-Ion Pairs Generation (10 mTorr, 500 W)

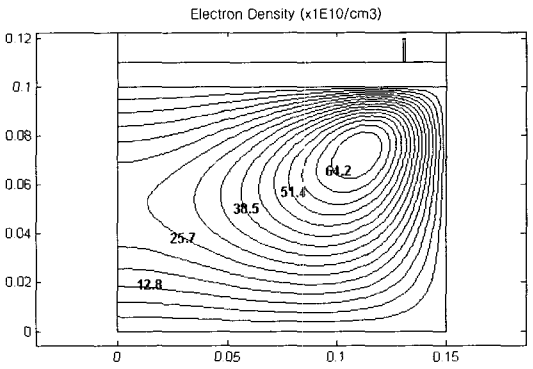

Fig. 4(a) Spatial Distribution of Electron Density(50 mTorr, 500W)

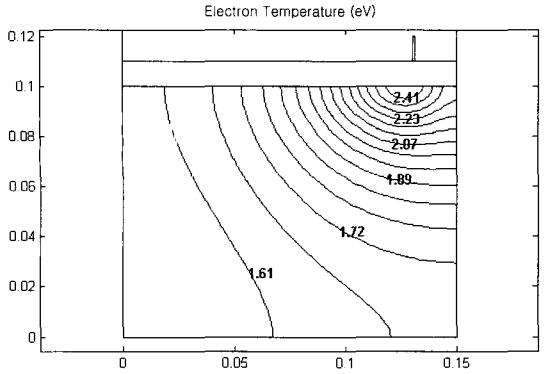

Fig. 4(b) Spatial Distribution of Electron Temperature (50 mTorr, 500 W)

region. The location of the maximum temperature and density moves toward the center of the chamber as compared with the single-turn case. These changes are mainly due to the alteration of the electric field and power absorption profile. Normalized plasma density profiles as a function of pressure for two different antenna configurations are displayed collectively in Fig. 6.

For the 5 mTorr and 10 mTorr conditions, the single-turn antenna shows better density uniformity.

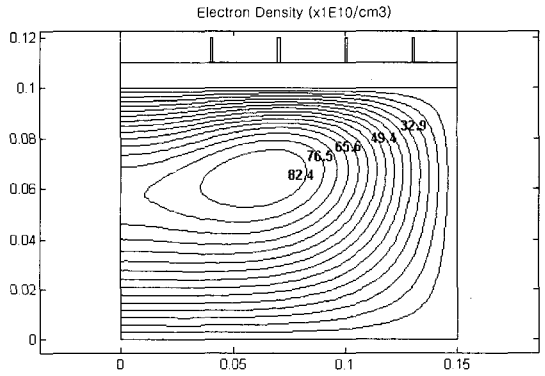

Fig. 5(a) Electron Density Distribution for Four-Turn Antenna (50 mTorr, 500W)

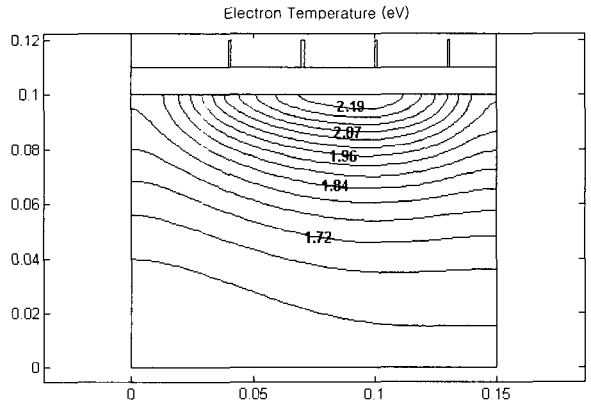

Fig. 5(b) Electron Temperature Distribution for Four-Turn Antenna (50 mTorr, 500W)

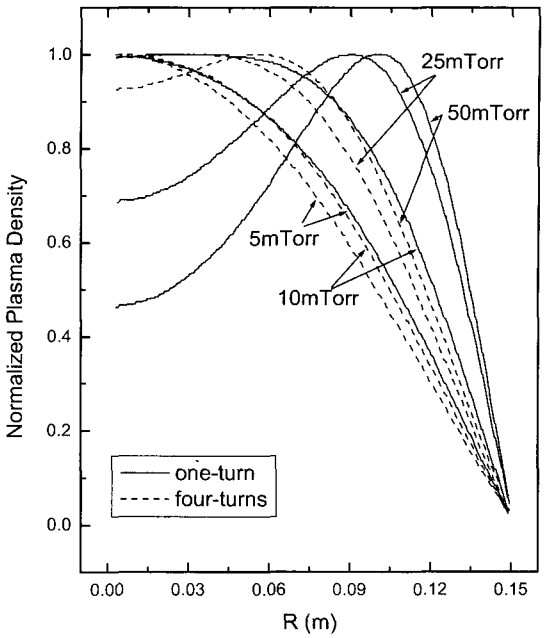

Fig. 6 Normalized plasma density along radial direction (Power 500W, z=5cm)

3.2 Pressure and power dependencies on plasma density and electron temperature

The effects of pressure on the plasma density and electron temperature are shown in Fig. 7(a). For a single-turn antenna, the maximum density monotonically increases with pressure. Density at the center of the chamber increases with pressure up to 10 mTorr, and then gradually

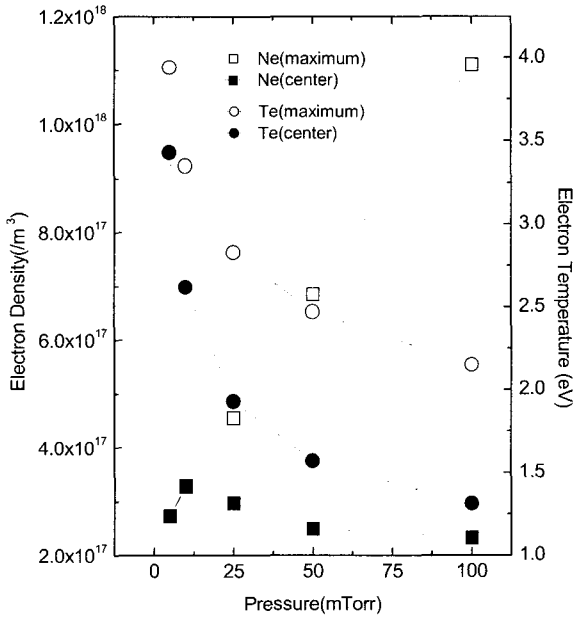

Fig. 7(a) Electron density and temperature as a function of pressure

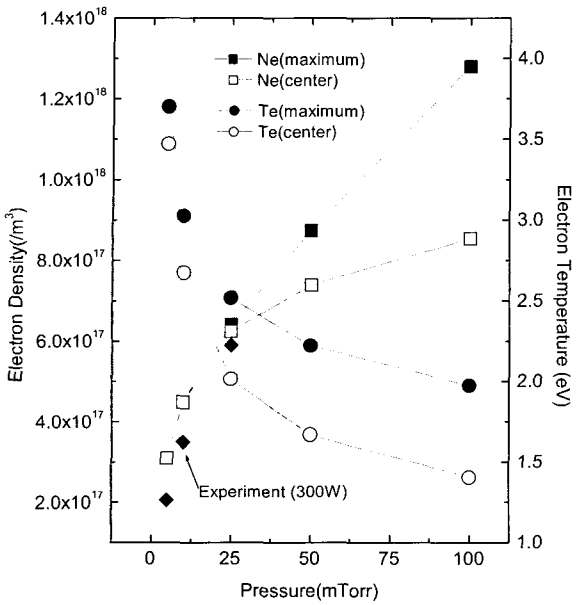

Fig. 7(b) Electron density and temperature as a function of pressure (500W, four-turn antenna)

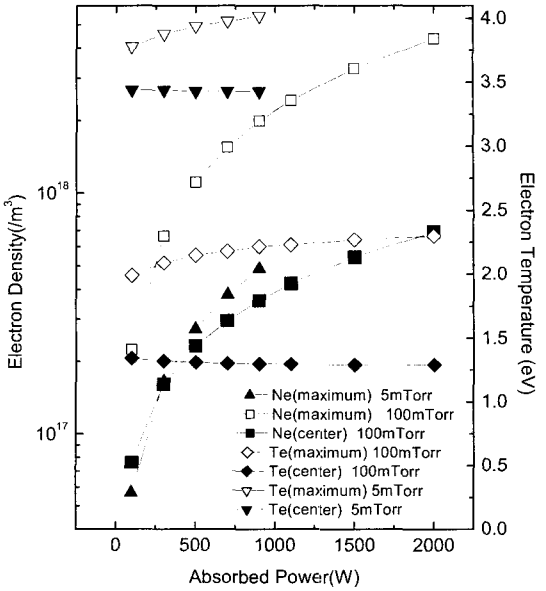

Fig. 8 Electron density and temperature as a function of input power (5mTorr and 100mTorr, one-turn antenna)

decreases. This is due to the fact that as the pressure increases the plasma becomes less diffusive and the density profile tends to follow the spatial distribution of electron-ion pair generation. On the other hand, for four-turn antenna as shown in Fig. 7(b), both maximum and center density increase with pressure because the location of the power absorption is shifted toward the center. The calculated result shows good agreement with the experimentally measured result [3].

Electron temperature decreases and the relative difference between maximum and center temperature increases with increasing pressure.

Input power dependencies are shown in Fig. 8. Densities increase almost linearly with power. While the peak electron temperature increases chamber remain constant.

3.3 Equivalent circuit parameters

Inductive power coupling between antenna and plasma is analogous basically to a transformer. The antenna acting as a primary coil and current loop of the plasma serves as the secondary coil.

From a practical point of view, the impedance seen from the antenna terminal (input port) is very important because a matching network should be designed based on this impedance. Furthermore, equivalent input resistance is closely related to the power transfer efficiency.

Fig. 9 shows the calculated value of resistance and reactance of the total load seen from the primary side. It should be noted that the resistance comes purely from the plasma itself since we do not account the conductivity of the copper coil. So without plasma, we can only have an induction field. In this situation the resistance seen from the input port is zero and the reactance depends on the geometry such as the location of the antenna. When there is plasma, conduction and polarization current (inductive in nature) arise, the effect of plasma on the resistance seen from the input port is expressed as a real part of the electric field at the location of the antenna. Terminal voltage can be obtained by the line integration along the antenna. We used the following approximation.[16]

$$V_r = 2\pi R E_{\theta r}$$

$$R_p = \frac{V_r}{I_0}$$

Here $E_{\theta r}$ is averaged over the antenna cross-section and R is the distance between the axis and center of the antenna. It is lumped element approximation, which is useful from a practical point of view. The validity of this treatment can be checked by comparing $P_r = \frac{1}{2} R_p I_0^2$ with the volume integral of the absorbed power. For all cases, the differences never exceed 1%. The reactance seen from the input port can be calculated by the same method.

$$V_i = 2\pi R E_{\theta i}$$

$$\omega L_p = \frac{V_i}{I_0}$$

The difference between the reactance with and without plasma simply tells the effective reactance of plasma. If the system is truly quasi-static, time average magnetic energy should be matched with the value of $P_r = \frac{1}{4} L_p I_0^2$. In our

cases, the discrepancies were found to be 2-3%.

When the pressure increases, the resistance increases and the reactance decreases. This means an improvement in power coupling. For a single-turn coil, power transfer efficiency η can be directly obtained from R_p as

$$\eta = \frac{R_p}{R_p + R_c}.$$

Here R_c is the resistance of the antenna coil at the operating frequency.

Several facts are responsible for the improvement of power coupling and efficiency with increasing pressure. Firstly, the real part of plasma conductivity increases due to the increment of collision frequency. Secondly, plasma density increases, which also leads to an enhancement of the conductivity value. Thirdly, the high-density region is closer to the primary coil at a higher pressure. This improves the mutual inductance between the primary and secondly coil. Fig. 10 shows power dependencies of equivalent impedances for low (5 mTorr) and high-pressure (100 mTorr) conditions. Since there is no significant difference in the spatial distribution of plasma densities according to the input power level, the alterations of R_p and ωL_s are mainly due to the global changes of conductivity. A more efficient power coupling can be obtained for higher power conditions. However, above a certain level of plasma density, R_p and power transfer efficiency decreases again as seen in the highest power condition at 100 mTorr. This characteristic has also been observed experimentally [3]. It can be easily understood if we consider the power transfer of the transformer, where no power can be transferred to both the open (extreme case of low conductivity) and short circuit (extreme case of high conductivity). The thickness of the rf window significantly affects R_p and ωL_s values. As shown in Fig. 9, it is evident that a thin window is advantageous to improving the power transfer efficiency.

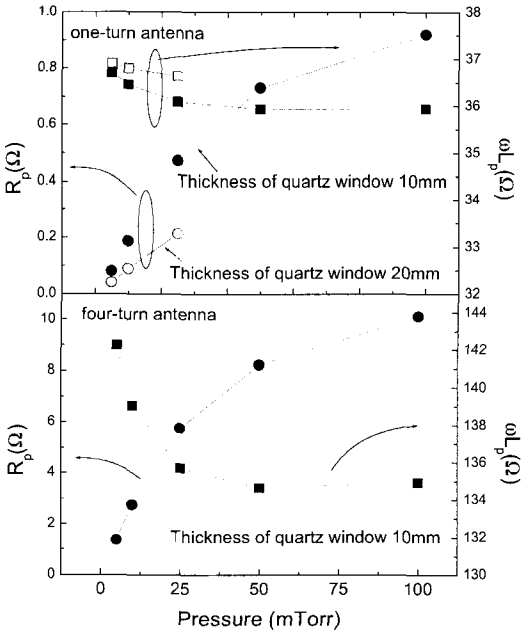

Fig. 9 Equivalent Impedance seen from antenna terminal – Pressure dependency (500W)

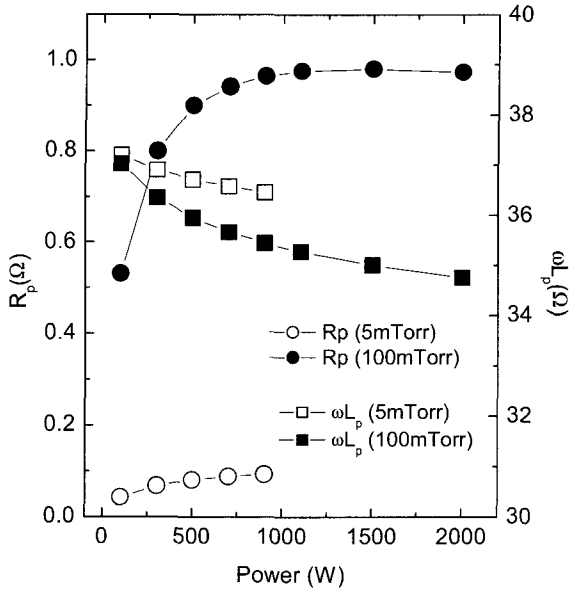

Fig. 10 Equivalent Impedance seen from antenna terminal – Power dependency

4.Conclusions

Spatial distributions of electron density and temperature of the planar type rf inductively coupled Argon plasma has been calculated from a simple model that includes ambipolar diffusion, energy conservation and quasi-static electromagnetic field analysis.

In addition to the effects of the typical process parameter, we presented the influences of design parameters such as antenna geometry and thickness of rf window on the characteristics of the plasma device. The calculated results agree qualitatively with experimental results. The equivalent circuit parameter reported in this paper can be used in designing the electrical interface between a plasma system and rf power amplifier.

Acknowledgement

This work was supported by Korean Research Foundation Grant (KRF-99-E00155).

References

[1] J. Givens, S Geissler, J. Lee, O. Cain, J Marks, P.Keswick and C. Cunningham "Selective Dry Etch-

ing in a High Density Plasma for 0.5um complementary MOS technology" *J. Vac. Sci. Technol.* B 12(1) pp.427-432, Jan. 1994.

[2] S.M. Rossnagel and J. Hopwood " Metal Ion Deposition from Ionized Magnetron Sputtering Discharge", *J. Vac. Sci. Technol.* B 12(1) pp.449-453, Jan. 1994.

[3] Ii-Dong Yang, Ho-Jun Lee, Ki-Woong Whang, "A Study on the Characteristics of Planar Type Inductively Coupled Plasma and it's Applications on the Selective Oxide Etching", *Journal of the Korean Vacuum Society*, 6(1) pp.92-98, Feb. 1997.

[4] J. Hopwood, C. R. Guarnieri, S. J. Whitehair, and J. J. Cuomo, "Electromagnetic fields in a radio-frequency induction plasma", *J. Vac. Sci. Technol.* A11(1), pp.147-151, Jan. 1993.

[5] J. Hopwood, C. R. Guarnieri, S. J. Whitehair, and J. J. Cuomo, "Langmuir probe measurements of a radio frequency induction plasma", *J. Vac. Sci. Technol.* A11(1), pp.152-156, Jan. 1993.

[6] M.A. Lieberman and A. J. Lichtenberg, *Principles of Plasma Discharges and Materials Processing*: John Wiley & Sons pp387-410, 1994.

[7] Peter L. G. Ventzek, Robert J. Hoekstra and Mark J. Kushner,"Two-dimsensional modeling of high density inductively coupled sources for materials processing", *J. Vac. Sci. Technol.* B 12(1) pp.461-477, Jan. 1994.

[8] R.A. Stewart, P. Vitello and D.B. Graves "Two-dimensional fluid model of high density inductively coupled plasma sources", *J. Vac. Sci. Technol.* B 12(1) pp.478-485, Jan. 1994.

[9] V.A.Godyak, R.B.Piejak and B.M. Alexandrovich "Electrical characteristics and electron heating mechanism of an inductively coupled argon discharge", Plasma Sources Sci. Technol. 3, pp169-176, 1994.

[10] Yu. M. Aliev, H. Schluter and A. Shivarova, *Guided-Wave-Produced Plasmas*: Springer-Verlag, pp7-28, 2000.

[11] A.D. Richards, B.E. Thompson, and Herbert H. Sawin, "Continuum modeling of argon radio frequency glow discharges", Applied Phys. Lett. 50(9) pp.489-491, Mar. 1987.

[12] Yuri P. Raizer, Gas Discharge Physics: Springer-Verlag, pp8-34, 1991.

[13] N.S.Yoon, S.S.Kim, C.S.Chang and D.K.Choi, "One-dimensional solution for Electron Heating in an Inductively Coupled Discharge", Phys. Rev. E, vol.54, no.1, pp757-768, 1997.

[14] N.S.Yoon, S.M.Hwang and D.K.Choi, "Two-dimensional non-local heating theory of planar-type inductively coupled plasma discharge", Phys. Rev. E, vol.55, no.6, pp7536-7549, 1997.

[15] COMSOL AB, "FEMLAB Reference Manual Ver2.2", 2001.

[16] Y.T. Kim, Y.S. Rho, H.S.Lee, and K.W. Whang "A Study on the characteristics of Inductively Coupled Plasma by Numerical Simulation" *Journal of the Korean Vacuum Society*, 3(4) pp.457-465, Feb. 1994.

Ho-Jun Lee received his Ph.D. degree in electrical engineering from Seoul National University, Korea, in 1996. From 1996 to 1998 he was a Visiting Researcher with the Venture Business Laboratory, Kyoto University, Japan. From 1999 to 2000 he was an Instructor with Uiduk University, Korea. Since 2001, he has been an Assistant Professor with the Dept. of Electrical Engineering, Pusan National University. His research interests are in engineering applications of plasmas, including flat panel display.

Dong-Hyun Kim received his B.E., M.E., and Ph.D. degrees in electrical engineering from Pusan National University, in 1984, 1998, and 2001, respectively. He was with the Technical Research Laboratory, Hyosung Industries Company, from 1998 to 1994. He is a Research Professor with the Institute of Computer and Information-Telecommunication, Pusan National University.

Chung-Hoo Park received his B.E. and M.E. degrees in electrical engineering from Pusan National University, Korea, in 1968 and 1974, respectively, and his Ph. D. degree from Kyushu University, Japan, in 1983. He is currently a Professor in the Dept. of Electrical Engineering, Pusan National University.